NOISE AND POSSIBLE LOSS OF LANDAU DAMPING THROUGH NOISE EXCITED WAKEFIELDS

S. V. Furuseth*[1], X. Buffat, CERN, 1211 Geneva 23, Switzerland
[1]also at EPFL, 1015 Lausanne, Switzerland

Abstract

The effect of transverse Landau damping in circular hadron colliders depends strongly on the bunch distribution. The bunches are often assumed to be Gaussian in the transverse dimensions, as it fits well to measurements and it is the expected effect of intra-beam scattering. However, a small change of the distribution can cause a loss of stability. We study the effect that external noise excites the transverse motion of the beam, which produces wakefields, which act back on the beam and cause a diffusion of incoherent particles. The diffusion is narrow in frequency space, and thus also in action space. Macroparticle simulations have shown a similar change of the distribution, which is only detectable in action space, not projected in position space. The narrow diffusion efficiently drills a hole in the stability diagram, at the location of the unstable mode, eventually leading to an instability. The advised mitigation technique is to reduce the drilling rate by operating with a stability margin.

INTRODUCTION

Synchrotrons, such as the Large Hadron Collider (LHC), are dependent on Landau damping for the beams to avoid self-amplified coherent oscillations. Landau damping is a physical process where an ensemble of harmonic oscillators, that would otherwise be unstable, is stabilized by a spread in the natural frequencies of the incoherent oscillators [1]. Therefore, it depends on the details of the beam and bunch distribution and the source of detuning that causes the spread in frequencies. It is common to study Landau damping with a linearized Vlasov equation, considering the effect of a small perturbation on top of an equilibrium perturbation.

In the LHC, multiple instances of instability have been observed that begin at a significant delay after the last modification of the machine configuration. The delay will be referred to as the latency of the instability. Latent instabilities have now also been reproduced in experiments in the LHC with a controlled noise source [2], detailed in Fig. 1. These instabilities cannot be attributed to a change of the machine configuration, and may therefore be attributed to a change of the beam distribution from the initial equilibrium distribution. Furthermore, given the dependence on the noise amplitude, the noise must be essential to the mechanism. It has previously been hypothesized, and checked with simulations, that the external noise excites the beam, which then is amplified by wakefields [3]. This mechanism can explain parts of the discrepancy between the predicted and operationally required octupole current in the LHC [4]. The goal of the work presented here is to describe the mechanism

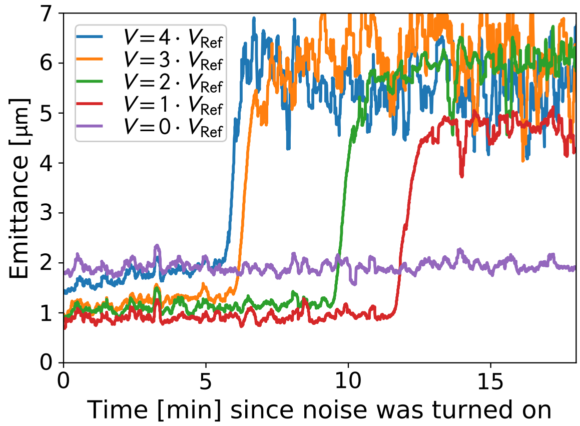

Figure 1: Emittance evolution of five bunches subject to a controlled noise source of relative magnitude given by the legend. The bunches went unstable in order of decreasing noise amplitude [2]. The six bunches not affected by noise, of which only one is displayed, did not go unstable in this configuration.

analytically as a wake-driven diffusion that causes a loss of Landau damping. The model will be used to better understand this mechanism, and to guide the search for optimal machine and beam parameters that mitigate this mechanism, relevant for the LHC and future projects.

THEORY

In this section, the (angular) frequencies ω are referred to instead of the tunes $Q = \omega/2\pi f_{\mathrm{rev}}$. The mathematical explanation of noise excited wakefields consists of 4 steps: (i) The wakefields drive eigenmodes with complex eigenfrequencies ω_m, found with the linearized Vlasov equation, assuming no tune spread and no noise; (ii) Due to the tune spread, the discrete mode mixes with the incoherent spectrum, and the complex eigenfrequencies are changed to Ω_m. If $\mathrm{Im}\{\Omega_m\} > 0$, the mode is already unstable. The interesting case is when $\mathrm{Im}\{\Omega_m\} < 0$; (iii) An external noise source of amplitude $\xi(t)$ as a function of time, kicks the bunches transversely. The noise drives the eigenmodes to finite amplitudes that depend on the noise amplitude and damping rate of the modes; (iv) The non-negligible noise excited wakefields act on the incoherent particles. By considering the kicks from the wakefields as a stochastic excitation in the framework of the Liouville equation, we will derive a diffusion equation modeling the distribution evolution driven by the noise excited wakefields.

* sondre.vik.furuseth@cern.ch

Wakefield eigenmodes – ω_m

The standard approach used to study beam stability is with a linearized Vlasov equation [5, 6]. This method considers the beam as a continuous distribution Ψ in phase space, consisting of a constant equilibrium distribution and a quickly oscillating perturbation

$$\Psi = \Psi_0 + \Psi_1. \tag{1}$$

One can similarly include the impedance as a perturbation in the Hamiltonian

$$\mathscr{H} = \mathscr{H}_0 + \mathscr{H}_{\text{wake}}, \tag{2}$$

where $\mathscr{H}_0$ models the unperturbed motion. The equilibrium distribution drives no dipolar wakefields. Thus, the wakefields are proportional to the distribution perturbation, $\mathscr{H}_{\text{wake}} \propto \Psi_1$.

The Liouville equation can be solved using the perturbed distribution in Eq. (1) and Hamiltonian in Eq. (2). One finds impedance normalized eigenmodes m_m with eigenvalues $\omega_m = \omega_0 + \Delta\omega_m$ and amplitudes $\chi_m(t)$, dependent on impedance, chromaticity and transverse feedback. The eigenmodes are complex functions of the longitudinal phase space coordinates. The distribution perturbation can be written as a sum over these modes

$$\Psi_1 = \sum_m \chi_m(t_0) e^{-i\omega_m(t-t_0)} m_m, \tag{3}$$

where i is the imaginary unit, and the importance of $\text{Im}\{\omega_m\}$ as a growth rate is highlighted. The amplitude of the individual modes are governed by

$$\ddot{\chi}_m m_m + \omega_m^2 \chi_m m_m = 0. \tag{4}$$

The frequency without impedance is $\omega_0 \in \mathbb{R}$. By moving the tune shift caused by the impedance over to the right hand side (RHS) one finds the impulse acted on the beam by the wakefields

$$\begin{aligned}\ddot{\chi}_m m_m + \omega_0^2 \chi_m m_m &= (\omega_0^2 - \omega_m^2) \chi_m m_m \\ &= \omega_m P_{\text{wake}} m_m. \end{aligned} \tag{5}$$

Damped eigenmodes – Ω_m

The discrete modes discussed in the previous subsection can be stabilized by Landau damping. This can be assessed by the stability diagram theory when all the (head-tail) modes can be treated independently, as is the case for the current LHC operation. In the weak head-tail approximation, the stability diagram in plane $j \in \{x, y\}$ corresponds to the curve in the complex plane defined by $\Delta\omega_{mj} \in \mathbb{C}$ in the dispersion relation [7]

$$\frac{-1}{\Delta\omega_{mj}} = \int_0^\infty \int_0^\infty \mathrm{d}J_x\, \mathrm{d}J_y \frac{J_j \dfrac{\mathrm{d}\Psi(J_x, J_y)}{\mathrm{d}J_j}}{\Omega_{mj} - \omega_j(J_x, J_y)}, \tag{6}$$

where the real part of $\Omega_{mj} = \omega_0 + \Delta\Omega_{mj} \in \mathbb{C}$ is scanned, while it has a vanishing positive imaginary part. This is the gray curve in Fig. 2. The source of detuning considered here is Landau octupoles [8]. The tune shift driven by the wakefields without detuning, $\Delta\omega_{mj}$, can be represented by a point in the same complex plane. If the point is below the stability diagram, it is stable, if it is above, it is unstable. The subscript j will be omitted from here on, when not important.

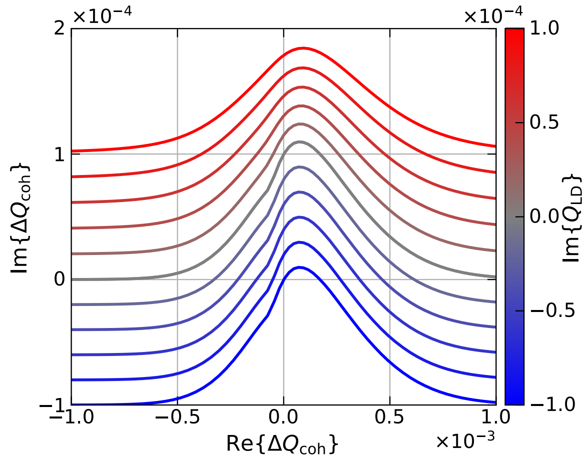

Figure 2: Curves at complex tune shift $\Delta Q_{\text{coh}} = \Delta\omega_m/2\pi f_{\text{rev}}$ of modes, when neglecting Landau damping, that end up with the same imaginary tune shift $\text{Im}\{Q_{\text{LD}}\} = \text{Im}\{\Omega_m\}/2\pi f_{\text{rev}}$, when including Landau damping. The grey curve is the stability diagram. The red curves with positive $\text{Im}\{Q_{\text{LD}}\} > 0$ are calculated directly with Eq. (6), while the blue curves are equal to the stability diagram shifted downwards by the corresponding $\text{Im}\{Q_{\text{LD}}\}$.

One can use Eq. (6) to find how the undamped tune shift $\Delta\omega_m$ changes due to the tune spread $\omega_j(J_x, J_y)$, by finding the corresponding Ω_m that maps to $\Delta\omega_m$. This is possible as long as the discrete mode remains unstable, $\text{Im}\{\Omega_m\} > 0$ [9].

Equation (6) cannot map a mode inside the stability diagram to Ω_m. When $\text{Im}\{\Omega_m\} = 0^+ \to 0^-$, the sign of $\text{Im}\{\Delta\omega_{mj}\}$ in Eq. (6) is flipped as well. In other words, there is a hole in the codomain of Eq. (6). The flipping has been found to be due to a mathematical choice, rather than based on physics [10].

The physics of what is happening when the most unstable modes are inside the stability diagram has previously not been given much attention [11, 12]. One reason why is that these modes are stabilized by Landau damping, and therefore are not a problem within linear Vlasov theory. However, due to noise, the dynamics of modes that are initially stable are crucial to determine whether the beams will remain stable. A similar problem has been discussed in plasma physics. Paraphrasing from [13], it was found for small distribution perturbations that "[A]n arbitrary initial distribution behaves (after a short transient time) like a superposition of [...] slightly damped plane waves, which do obey the dispersion relation". We assume for now the same to be true in a particle beam.

A new algorithm must be designed to calculate the complex frequencies of the Landau damped modes that reside inside the stability diagram. For the results that will be presented here, the hypothesis has been made that one can extend the mapping in Eq. (6) linearly from $\mathrm{Im}\{\Omega_m\} = 0^+$ into the area where the imaginary part is negative. This is illustrated by the blue lines in Fig. 2. This approach neglects the continuous spectrum of the beam that is believed to be negligible after a short transient time, when the mode is close to the stability threshold. Thus, this method is only believed to be accurate when the least stable modes are close to the stability diagram. This is the main region of interest in this paper.

Noise excited eigenmodes

The unavoidable noise in the accelerator has been neglected so far for beam stability considerations. The noise can be modeled as an additional stochastic perturbation to the Hamiltonian in Eq. (2)

$$\mathcal{H} = \mathcal{H}_0 + \mathcal{H}_{\mathrm{wake}} + \mathcal{H}_{\mathrm{noise}}. \tag{7}$$

The external noise is expected to act at low frequencies and thus to be dipolar in nature (i.e. affecting all particles along the bunch equally). It will be included as a stochastic impulse $\xi(t)$, of zero mean, $\langle \xi(t) \rangle = 0$ and singular autocorrelation $\langle \xi(t)\xi(s) \rangle = \sigma^2 \delta(t - s)$. It can be decomposed as $\xi(t) = \xi(t_c)\Xi(z)$, where $\xi(t_c)$ is the noise amplitude at the core of the bunch longitudinally, while $\Xi(z)$ is a normalized function across the length of the bunch. Under the assumption of dipolar noise, $\Xi(z)$ will be a constant. The impact of the noise on a bunch can be integrated in quadrature into a single kick per turn of variance $\sigma^2_{\mathrm{ext}} = \tau\sigma^2$, where $\tau = 1/f_{\mathrm{rev}}$ is the revolution period of the machine. By the Plancherel theorem, the power spectral density of the noise is given by [14]

$$|\mathcal{F}[\xi]|^2(\omega) = \begin{cases} \dfrac{\sigma^2_{\mathrm{ext}}}{\tau} & , \omega \in [0, \pi f_{\mathrm{rev}}] \\ 0 & , \text{otherwise.} \end{cases} \tag{8}$$

The left hand side is the absolute value squared of the Fourier transform of the noise signal as a function of the angular frequency.

The impact of the external noise on the eigenmodes can be found by including the noise on the RHS of Eq. (4) and multiplying from the left with $\overline{m_m}$, and taking the average over the longitudinal distribution, as

$$\ddot{\chi}_m + \omega_m^2 \chi_m = \omega_m \langle \overline{m_m}\Xi \rangle \, \xi(t_c) = \omega_m \eta_m \xi(t_c). \tag{9}$$

Thus, mode m_m will on average be affected proportionally to its dipolar moment η_m. The mode is modeled as a stochastically driven damped harmonic oscillator, and one can easily find that the frequency spectrum of χ_m is

$$\mathcal{F}[\chi_m](\omega) = \frac{\Omega_m \eta_m \mathcal{F}[\xi](\omega)}{\Omega_m^2 - \omega^2}, \tag{10}$$

centred and peaked at the frequency of the mode, Ω_m. In this paper, the considered noise spectrum is flat. However, in a real machine, what matters is the noise spectrum close to the mode frequency. Since the mode is damped, $\mathrm{Im}\{\Omega_m\} \neq 0$, its frequency spectrum is free of singularities.

Wakefield driven diffusion

The main question that remains is how the noise excited damped modes affect the incoherent particles. The incoherent particles in a bunch, will in either transverse plane be described by their normalized canonical coordinates [15]

$$\begin{aligned} y &= \frac{Y}{\sqrt{\beta\varepsilon_0}} = \sqrt{2J}\cos(\phi), \\ p &= -\frac{1}{\sqrt{\beta\varepsilon_0}}\left(\alpha Y + \beta\frac{\mathrm{d}Y}{\mathrm{d}s}\right) = -\sqrt{2J}\sin(\phi), \end{aligned} \tag{11}$$

where Y is the offset from the design orbit, s is the position in the beamline, α and β are the Twiss parameters, ε_0 is the initial beam emittance and ϕ is the canonical conjugate of J, which is the normalized absolute particle action, given in units of ε_0.

In the case when $\phi = \omega_0 t$, where ω_0 is the constant incoherent betatron frequency, and the particle receives impulses $\Delta p(t)$, the Hamiltonian can be written as

$$\mathcal{H} = \omega_0 J - y\Delta p = \omega_0 \frac{y^2 + p^2}{2} - y\Delta p, \tag{12}$$

such that Hamilton's equations read

$$\dot{y} = \omega_0 p, \quad \dot{p} = -\omega_0 y + \Delta p, \tag{13}$$

which lead to the following equation of motion

$$\ddot{y} + \omega_0^2 y = \omega_0 \Delta p. \tag{14}$$

In our case, the sources of the impulses Δp are the external noise and wakefields,

$$\Delta p = \xi + P_{\mathrm{wake}} = \xi + \sum_m \frac{1}{\omega_m}(\omega_0^2 - \omega_m^2)\chi_m. \tag{15}$$

The first term on the RHS will be referred to as the direct noise term, while the second term will be referred to as the indirect noise term. The direct impact on beam stability of the external noise was found to be negligible for the LHC in [16].

Here, we will consider the second term, the impulses from the noise excited wakefields. This will be considered by the perturbed Hamiltonian in Eq. (2), renamed as

$$\mathcal{H} = \mathcal{H}_0(J) + \mathcal{H}_1(\phi, J) = \mathcal{H}_0(J) - yP_{\mathrm{wake}}, \tag{16}$$

consisting of $\mathcal{H}_0$ governing the unperturbed non-stochastic motion, and the perturbation $\mathcal{H}_1$ containing the stochastic forces. It is important that $\mathcal{H}_0$ only depends on the actions, not the phases ϕ of the particles. If the stochastic forces are sufficiently weak, and thus can be modeled as a perturbation, they drive a diffusion that can be modeled by [17, 18]

$$\frac{\partial \Psi_{\mathrm{eq}}}{\partial t} = \frac{\partial}{\partial J}\left[J D_{\mathrm{wake}} \frac{\partial \Psi_{\mathrm{eq}}}{\partial J}\right]. \tag{17}$$

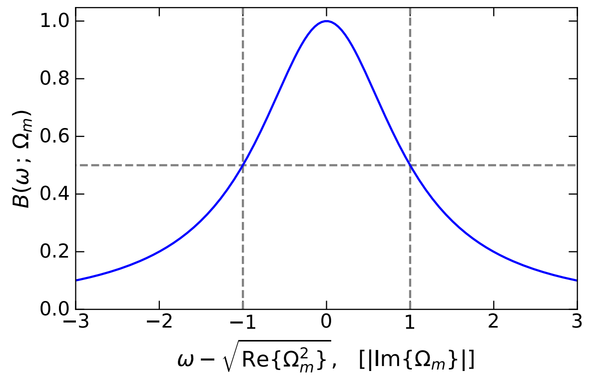

Figure 3: Shape of the diffusion coefficient due to a single stable wake driven mode, given by Eq. (19b).

The wakefield driven diffusion coefficient D_{wake} is given by

$$
\begin{aligned}
D_{\text{wake}}(\omega) &= \frac{1}{2J}\left\langle \frac{\partial \mathcal{H}_1}{\partial \phi}(t)\frac{\partial \mathcal{H}_1}{\partial \phi}(s)\right\rangle \\
&= \frac{1}{2}|\mathcal{F}[P_{\text{wake}}]|^2(\omega),
\end{aligned} \tag{18}
$$

where the brackets signify an expectancy value, the bar signifies a complex conjugation required to get a real diffusion coefficient, and P_{wake} is stochastic since the beam continuously is excited by the stochastic noise. The diffusion coefficient is a function of the angular frequency of the particles.

The absolute value of the Fourier transform squared in Eq. (18) is the power spectral density of the impulse from the wakefields. In the interesting regime of this work, the modes are uncoupled, and the power of the different modes can be added in quadratures to express the diffusion coefficient as

$$D_{\text{wake}}(\omega) = \sum_m \frac{\eta_m^2 \sigma_{\text{ext}}^2 |\Delta\omega_m|^2}{2\tau \text{Im}\{\Omega_m\}^2} B(\omega) C, \tag{19a}$$

$$B(\omega) = \frac{\text{Im}\{\Omega_m^2\}^2}{(\text{Re}\{\Omega_m^2\} - \omega^2)^2 + \text{Im}\{\Omega_m^2\}^2}, \tag{19b}$$

$$C = \frac{\text{Re}\{\omega_m\}\omega_0 + |\Delta\omega_m|^2/4}{\text{Re}\{\Omega_m\}^2} \cdot \frac{|\Omega_m|^2}{|\omega_m|^2} \approx 1. \tag{19c}$$

The B-function, which is illustrated in Fig. 3, defines the shape of the diffusion coefficient as a function of the incoherent angular frequency ω. In the limit $|\Delta\Omega_m| \ll |\omega_0|$, $B(\omega)$ has a maximum of 1 and half width $|\text{Im}\{\Omega_m\}|$ at half maximum. The C-function consists of additional factors that follow if one includes more than the first order terms. It is close to 1 for all realistic configurations considered here. In most cases, one mode will be dominant and be the main driver of diffusion within the bunch distribution.

The frequency dependent diffusion coefficient in Eq. (19) becomes amplitude dependent due to the amplitude dependent detuning as

$$D_{\text{wake}}(J_x, J_y) = D_{\text{wake}}[2\pi f_{\text{rev}} Q(J_x, J_y)]. \tag{20}$$

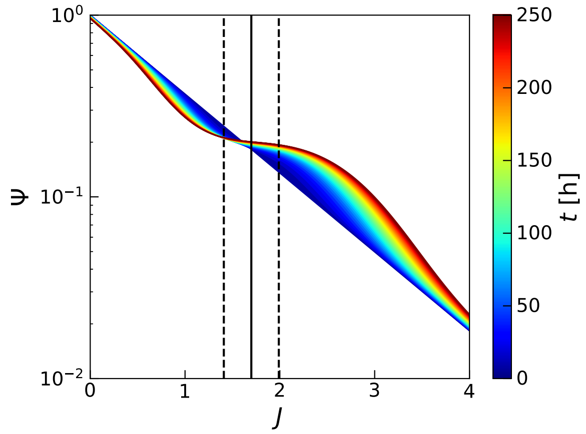

Figure 4: Evolution of transverse distribution due to wake driven diffusion with detuning only dependent on the action in the same plane. The actions at half maximum of the diffusion coefficient is marked by the vertical dashed lines. This example is intended for explaining the distribution evolution only.

In this paper, we are interested in the detuning caused by Landau octupoles, which in plane j can be expressed as [8]

$$Q_j = Q_{0j} + a_j J_x + b_j J_y, \tag{21}$$

excluding the negligible tune shift caused by the perturbations in Eq. (7).

A qualitative understanding of what this diffusion does to the beam, can be acquired already from the expression for the diffusion coefficient in Eq. (19). Assuming noise and diffusion in the horizontal plane only, the half width of the diffusion coefficient in the horizontal action coordinate will be $W_J = \text{Im}\{\Omega_m\}/2\pi f_{\text{rev}} a_x$. The diffusion will lead to a local flattening of the distribution, and as it is the derivative of the distribution function that appears in the dispersion integral in Eq. (6), a local loss of Landau damping can be expected. The flattening process will be faster for a smaller W_J, assuming the same maximum. For sufficiently large W_J, the diffusion will be approximately uniform for all actions, and only lead to an emittance growth, not a qualitative change of the distribution.

NUMERICAL METHOD

The diffusion equation in Eq. (17) must be solved numerically. The results that will be presented later have been produced with a finite volume method (FVM) solver implemented in `PyRADISE` (Python RAdial DIffusion and Stability Evolution) [16]. The two dimensional action space has been discretized into a 500 × 500 grid going from 0 to $J_{\text{max}} = 18$. It has been assumed that a single mode is dominant. In reality, changes in the distribution will lead to a change of the frequency of the least stable mode, and consequently a change of the dependence of diffusion on the action. This evolution has not been calculated during the diffusion process in the numerical results presented in this paper. In other words, the diffusion coefficients are kept constant throughout the solving process. Given the shape of the diffusion coefficient in Eq. (19), and linear detuning driven by Landau octupoles, the diffusion will lead to a local flattening of the distribution, which is exemplified and exaggerated for $b_j = 0$ in Fig. 4.

The FVM solver gives as output the evolving distribution Ψ_k at discrete times t_k. For each of these distributions, the stability diagram is calculated using a numerical trapezoidal integrator in `PySSD` [19], which has been imported in `PyRADISE`. If the stability diagram changes enough, so that the least stable mode is outside and above it, the bunch will be considered to have become unstable with a latency.

RESULTS

The following results consider the change of distribution and corresponding change of the stability diagram according to `PyRADISE`. There are small variations between the configurations. The detuning coefficients in Eq. (21) are always $a_x = a_y = 5 \times 10^{-5}$ and $b_x = b_y = -3.5 \times 10^{-5}$. The product of the noise amplitude and the dipole moment of the considered least stable mode in the horizontal plane is kept at $\sigma_{\text{ext}}\eta_m = 5 \times 10^{-6}$. The noise in the vertical plane has been kept equal to zero. The revolution frequency is that of the LHC, $f_{\text{rev}} = 11.245$ kHz.

The first configuration includes a least stable mode of undamped coherent tune shift $\Delta Q_{\text{coh}} = -10^{-4} + 10^{-5}\text{i}$. Due to Landau damping, this mode has been changed to $\Delta Q_{\text{LD}} = -6.98 \times 10^{-5} - 1.17 \times 10^{-5}\text{i}$, according to the algorithm illustrated in Fig. 2. The evolution of the distribution and stability diagram is presented in Fig. 5. The change of the distribution after 10 min is a local flattening horizontally at the actions corresponding to $Q_x(J_x, J_y) = Q_{\text{LD}}$, equivalent to the flattening in Fig. 4. There is a change of the stability diagram at the real tune shift of the least stable

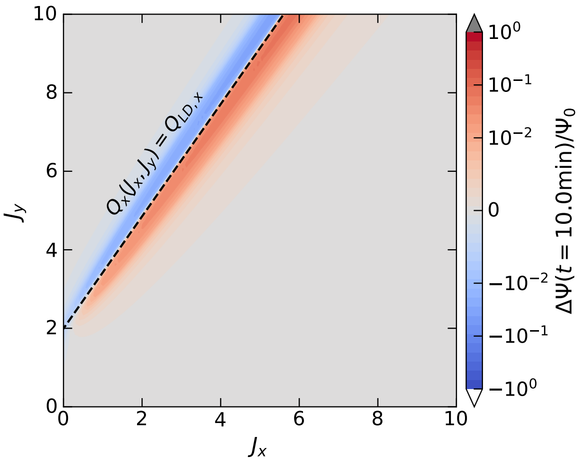

(a)

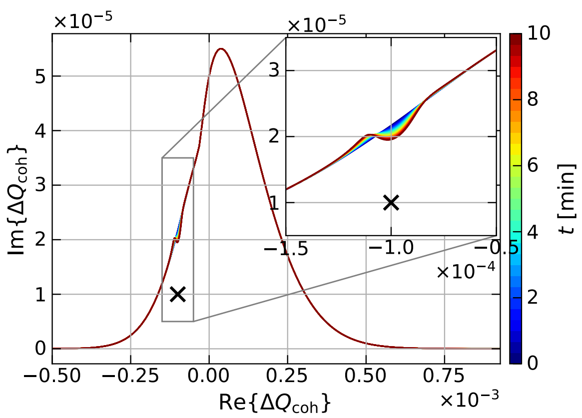

(b)

Figure 5: Evolution of distribution in 10 min in (a) and stability diagram in (b), due to diffusion driven by wakefields. The dashed line in (a) marks the actions where $Q_x(J_x, J_y) = Q_{\text{LD}}$. The cross at $\Delta Q_{\text{coh}} = -10^{-4} + 10^{-5}\text{i}$ in (b) marks the location of the least stable mode.

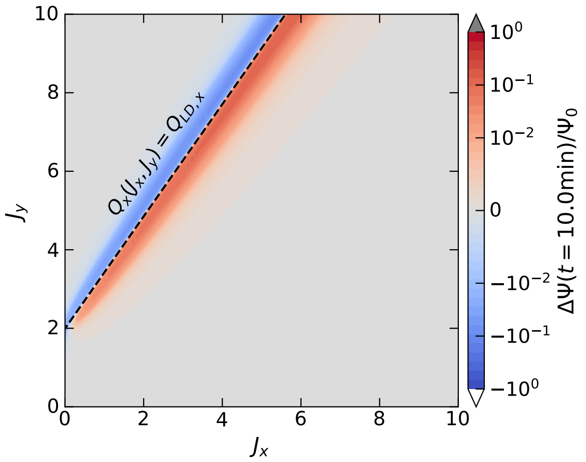

(a)

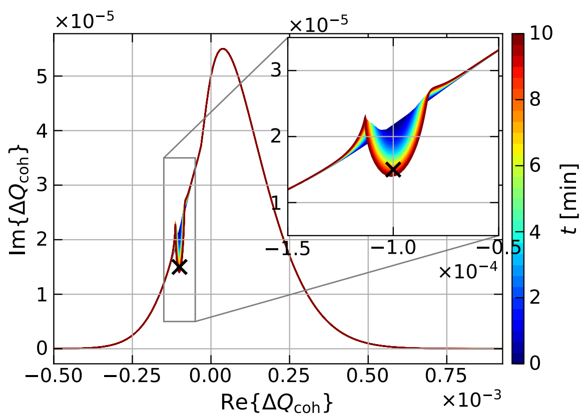

(b)

Figure 6: Evolution of distribution in 10 min in (a) and stability diagram in (b), due to diffusion driven by wakefields. The dashed line in (a) marks the actions where $Q_x(J_x, J_y) = Q_{\text{LD}}$. The cross at $\Delta Q_{\text{coh}} = -10^{-4} + 1.5 \times 10^{-5}\text{i}$ in (b) marks the location of the least stable mode.

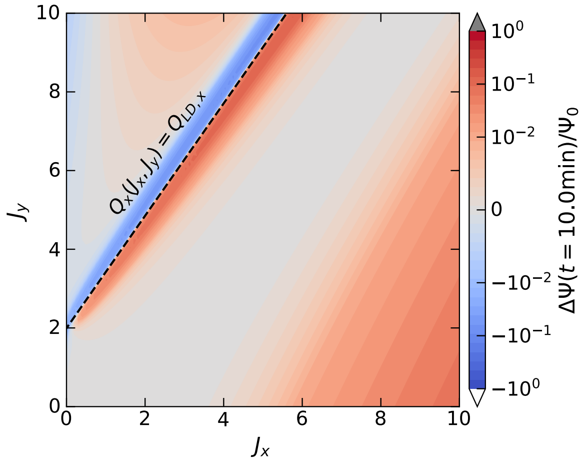

(a)

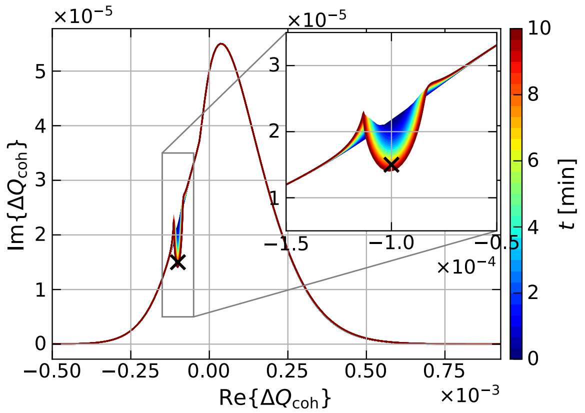

(b)

Figure 7: Evolution of distribution in 10 min in (a) and stability diagram in (b), due to diffusion driven by wakefields and the external noise directly. The dashed line in (a) marks the actions where $Q_x(J_x, J_y) = Q_{\text{LD}}$. The cross at $\Delta Q_{\text{coh}} = -10^{-4} + 1.5 \times 10^{-5}\text{i}$ in (b) marks the location of the least stable mode.

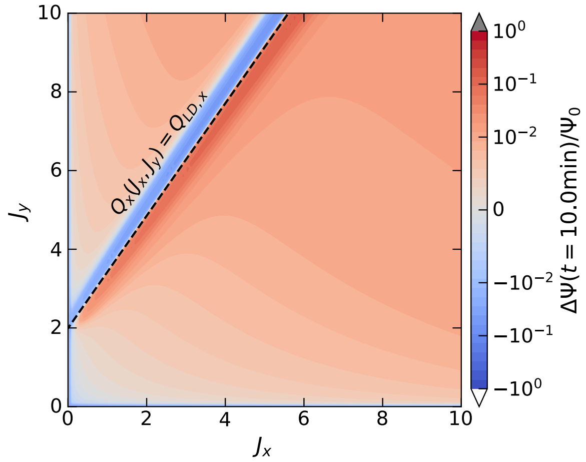

(a)

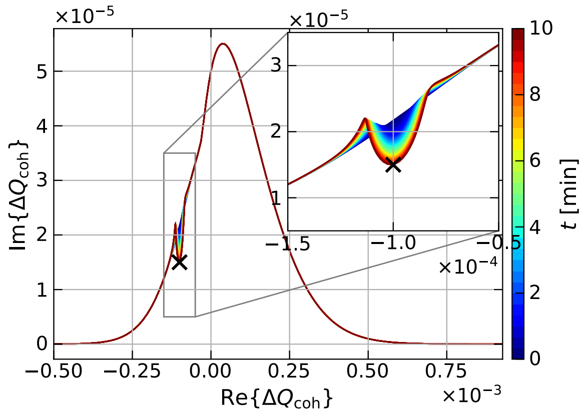

(b)

Figure 8: Evolution of distribution in 10 min in (a) and stability diagram in (b), due to diffusion driven by wakefields and intra-beam scattering. The dashed line in (a) marks the actions where $Q_x(J_x, J_y) = Q_{\text{LD}}$. The cross at $\Delta Q_{\text{coh}} = -10^{-4} + 1.5 \times 10^{-5}\text{i}$ in (b) marks the location of the least stable mode.

mode, but the mode is still well within the stability diagram after 10 min.

In the second configuration, the least stable mode has been shifted to $\Delta Q_{\text{coh}} = -10^{-4} + 1.5 \times 10^{-5}\text{i}$, closer to the stability threshold. Due to Landau damping, this mode has been changed to $\Delta Q_{\text{LD}} = -6.98 \times 10^{-5} - 6.70 \times 10^{-6}\text{i}$, with a smaller absolute imaginary part than in the first configuration. The evolution of the distribution and stability diagram is presented in Fig. 6. Due to the weaker damping of the mode, the drilling of a hole in the stability diagram is more efficient, and the least stable mode would have become unstable after approximately 8 min. This mechanism is thus able to drive instabilities with latencies of the same order of magnitude as those measured in the LHC in Fig. 1.

So far, only the diffusion due to the noise excited wakefields has been studied. Other types of diffusion may be able to counteract the local flattening and thereby increase the latency or even prevent the instability. In this third configuration, the diffusion driven by the direct noise term in Eq. (15) has been included. This diffusion was studied in detail in [16] and was found to not be detrimental for stability. Including a damper gain corresponding to a damping time of $\tau_g = 20$ turns and external noise amplitude $\sigma_{\text{ext}} = 10^{-3}$, the evolution of the distribution and stability diagram is presented in Fig. 7. The additional diffusion is zero for actions such that $Q_x(J_x, J_y) = \langle Q_x(J_x, J_y) \rangle$, which is close to the tune of the least stable mode. The instability in this configuration occurs 1.3% later, compared to the case without the direct noise term that was illustrated in Fig. 6. In other words, the direct noise term has negligible stabilizing impact in this configuration.

Finally, the uniform diffusion expected due to intra-beam scattering will be considered. A diffusion corresponding to an emittance growth of 2 % h^{-1} has been included in both planes, and the diffusion due to the direct noise term in Eq. (15) has been removed. The evolution of the distribution and stability diagram is presented in Fig. 8. There is now a weak nonzero diffusion at all actions, but it has not completely counteracted the local flattening close to Q_{LD}. The least stable mode would have become unstable after approximately 10 min, 26% later than without the uniform diffusion.

MITIGATION

Noise excited wakefields drive a narrow diffusion in frequency that leads to the drilling of a hole in the stability diagram. There are several possible approaches one can take to mitigate the total drilling. First of all, one should minimize the time spent in transient phases close to the instability threshold. In a collider, the most critical phase is between the end of the energy ramp and the start of collisions. In the LHC the bunches require stabilization by Landau octupoles alone during this phase. Second of all, one should minimize the drilling rate. The magnitude of the diffusion coefficient in Eq. (19a) is proportional to $\sigma_{\mathrm{ext}}^2\eta_m^2|\Delta\omega_m|^2/|\mathrm{Im}\{\Omega_m\}|^2$. To reduce the diffusion, one can therefore act with equal success on either of these factors: (i) Minimize the noise acting on the beam in the machine; (ii) Operate in a regime where $\eta_m \ll 1$. In a machine with only dipolar noise, one should therefore operate with positive chromaticity (above transition) to stabilize the dipolar modes, as is common; (iii) Minimize the machine impedance to limit $|\Delta\omega_m|$. This is already desired to minimize the initial stability threshold, neglecting that the diffusion changes the distribution; (iv) Maximize $|\mathrm{Im}\{\Omega_m\}|$, by operating with a stability margin. This was further motivated by the numerical results.

Further mitigation techniques can be discussed based on the numerical calculations. Incoherent noise as intra-beam scattering or synchrotron radiation can to a certain extent counteract the drilling. This may explain why such latent instabilities have not been reported before, neither in lepton machines, nor in low-energy hadron machines. Since the drilling of the hole is localized at a certain frequency, it is possible to gradually change the current in the Landau octupoles, to avoid continuously flattening the distribution at the same actions. However, this must be balanced with the goal of maximizing $|\mathrm{Im}\{\Omega_m\}|$. It is also possible to consider increasing the ratio b_j/a_j of the detuning coefficients, such that the width of the diffusion coefficient in action space is increased while not reducing the overall Landau damping.

If it is not possible to mitigate this mechanism with the techniques proposed so far, one must consider other sources of detuning. In addition to limiting the time before the beams are put in collision in a collider, one can try one of the following: electron-lens [20], enhanced octupole detuning due to the telescopic index [21], and wires designed to counteract beam-beam detuning [22].

CONCLUSION

Instabilities of high latencies have been observed in the LHC, both in regular operation and in dedicated experiments. In this paper, we have shown that such instabilities can develop in high-energy hadron machines with noise and impedance, by gradually changing the distribution. The key mechanism is driven by an external source of noise that excites the beam, which in return affects incoherent particles through wakefields. These wakefields cause diffusion in a narrow frequency range centred at the eigenfrequency of the least stable wake driven coherent mode. This diffusion efficiently drills a hole in the stability diagram at the eigenfrequency of the corresponding mode. The recommended mitigation technique is to reduce the drilling rate, by minimizing the maximum of the diffusion coefficient $D \propto \sigma_{\mathrm{ext}}^2\eta_m^2|\Delta\omega_m|^2/|\mathrm{Im}\{\Omega_m\}|^2$. Other sources of diffusion, as the direct external noise and intra-beam scattering, can increase the latency, but does not necessarily mitigate the drilling process completely.

It is believed that the mechanism presented here, diffusion driven by noise excited wakefields, is important in understanding the troubling observations in the LHC. Many aspects of this mechanism require and deserve further investigation. The description of the Landau damped modes deserve further studies. The chromatic tune shift of the incoherent particles remains to be included, and is believed to be important in understanding the diffusion of a mode close to a sideband of the main tune. The numerical method will be improved to self-consistently calculate the diffusion coefficient as the distribution evolves. Other types of noise, such as the crab-cavity amplitude noise, should be studied, as it is expected to drive head-tail modes as efficiently as dipolar noise drives dipolar modes. Finally, it will be of interest to compare quantitatively the latencies predicted with this theory to instability latencies measured in the LHC.

ACKNOWLEDGEMENTS

The authors would like to thank Nicolas Mounet for discussions on the dynamics of the modes that are stabilized by Landau damping, Armando Bazzani for discussions on the diffusion, and Elias Métral and Gianluigi Arduini for feedback on this manuscript. This research was supported by the HL-LHC project.

REFERENCES

[1] J. Rees and A. Chao, “Landau Damping Revisited”, SLAC National Accelerator Laboratory, Menlo Park, California, Rep. SLAC-PUB-13469, Nov. 2008.

[2] S. V. Furuseth, D. Amorim, S. A. Antipov, X. Buffat, N. Mounet, E. Métral, T. Pieloni, B. Salvant, and C. Tambasco, “Instability Latency in the LHC”, in *Proc. IPAC'19*, Melbourne, Australia, May 2019, pp. 3204–3207. doi:10.18429/JACoW-IPAC2019-WEPTS044

[3] X. Buffat, “Transverse beams stability studies at the Large Hadron Collider”, Ph.D. thesis, Inst. of Physics, École poly-

technique fédérale de Lausanne, Lausanne, Switzerland, 2015, CERN-THESIS-2014-246. doi:10.5075/epfl-thesis-6321

[4] X. Buffat, G. Arduini, D. Amorim, S. Antipov, N. Biancacci, L. Carver, S. V. Furuseth, G. Iadarola, K. Li, L. Mether , E. Métral, N. Mounet, A. Oeftiger, A. Romano, G. Rumolo, B. Salvant, M. Schenk, T. Pieloni, and C. Tambasco, "Transverse instabilities", in *Proc. 9th LHC Operations Evian Workshop*, Evian, France, Jan 2019. `https://indico.cern.ch/event/751857/contributions/3259409`

[5] A. A. Vlasov, "On the kinetic theory of an assembly of particles with collective interaction", *Russ. Phys. J.* **9**, pp. 25–40, 1945.

[6] N. Mounet, "Vlasov solvers and macroparticle simulations", in *CERN Yellow Reports: Conference Proceedings* **1**, p. 77, 2018, Rep. CERN-2018-003-CP. doi:10.23732/CYRCP-2018-001.77

[7] J. S. Berg and F. Ruggiero, "Landau damping with two-dimensional betatron tune spread", CERN, Geneva, Switzerland, Rep. CERN-SL-AP-96-071-AP, Dec. 1996.

[8] J. Gareyte, J. P. Koutchouk, and F. Ruggiero, "Landau damping, dynamic aperture and octupoles in LHC", CERN, Geneva, Switzerland, Rep. CERN-LHC-PROJECT-REPORT-091, Feb. 1997.

[9] J. L. Laclare, "Introduction to coherent instabilities – Coasting beam case", CERN, Geneva, Switzerland, Rep. CERN-85-19-V-2, 1985. doi:10.5170/CERN-1985-019-V-2.377

[10] N. Mounet, "Landau-damped modes - To be or not to be, that is the question", in CERN/BE-ABP-HSC section meeting, Jan. 2020, unpublished. `https://indico.cern.ch/event/874562/contributions/3689477/` (accessed: 2020-3-6).

[11] Y. H. Chin, "Nonlinear perturbation approach to bunch lengthening and blow-up of energy spread", *Nuclear Instruments and Methods in Physics Research Section A: Accelerators, Spectrometers, Detectors and Associated Equipment* **226**, pp. 223–249, Oct. 1984. doi:10.1016/0168-9002(84)90037-8

[12] Y. H. Chin, K. Satoh, and K. Yakoya, "Instability of a bunched beam with synchrotron-frequency spread", *Particle Accelerators* **13**, pp. 45–66, 1983, Rep. KEK-82-18.

[13] N. G. Van Kampen, "On the theory of stationary waves in plasmas", *Physica* **21**, pp. 949–963, 1955. doi:10.1016/S0031-8914(55)93068-8

[14] M. Plancherel, "Contribution à l'étude de la représentation d'une fonction arbitraire par les intégrales définies", *Rendiconti del Circolo Matematico di Palermo* **30** (1), pp.289–335, 1910. doi:10.1007/BF03014877

[15] A. Wolski, *Beam dynamics in high energy particle accelerators*. London, England: Imperial College Press, 2014.

[16] S. V. Furuseth and X. Buffat, "Long-term evolution of Landau damping in the presence of transverse noise, feedback, and detuning", *Phys. Rev. Accel. Beams* **23**, 034401, 2020. doi:10.1103/PhysRevAccelBeams.23.034401

[17] A. Bazzani, S. Siboni, and G. Turchetti, "Diffusion in Hamiltonian systems with a small stochastic perturbation", *Physica D* **76**, pp. 8–21, 1994. doi:10.1016/0167-2789(94)90246-1

[18] A. Bazzani and L. Beccaceci, "Diffusion in Hamiltonian systems driven by harmonic noise", *J. Phys. A: Math. Gen.* **31**, pp. 5843–5854, 1998. doi:10.1088/0305-4470/31/28/004

[19] X. Buffat, W. Herr, N. Mounet, T. Pieloni, and S. White, "Stability diagrams of colliding beams in the Large Hadron Collider", *Phys. Rev. ST Accel. Beams* **17**, 111002, 2014. doi:10.1103/PhysRevSTAB.17.111002

[20] V. Shiltsev, Y. Alexahin, A. Burov, and A. Valishev, "Landau Damping of Beam Instabilities by Electron Lenses", *Phys. Rev. Lett.* **119**, 134802, 2017. doi:10.1103/PhysRevLett.119.134802

[21] S. Fartoukh, "Achromatic telescopic squeezing scheme and its application to the LHC and its luminosity upgrade", *Phys. Rev. ST Accel. Beams* **16**, 111002, 2013. doi:10.1103/PhysRevSTAB.16.111002

[22] S. Fartoukh, A. Valishev, Y. Papaphilippou, and D. Shatilov, "Compensation of the long-range beam-beam interactions as a path towards new configurations for the high luminosity LHC", *Phys. Rev. ST Accel. Beams* **18**, 121001, 2015. doi:10.1103/PhysRevSTAB.18.121001